While dissociation analysis provided consistent data, there was always some residual ^{125}IhCG which remained bound to the NC even after several days of dissociation. The extent of dissociation observed ranged between 50 and 80%. However, the rate constants obtained were independent of the extent of the dissociation. It was generally observed that when the ^{125}IhCG was freshly prepared, or had high specific activity the dissociation was much better (70–80%), and reduced to 50% with storage. The reason for this lack of dissociation of a part of the ^{125}IhCG is now known. Infact very limited (Ag–Ab) dissociation of macromolecular complex is frequently observed in the BIAcore experiments also[10–12], and this apparent nonreversibility is not unique for the radiolabel.

In summary, we successfully adopted NC as an alternate support for adsorption of MAbs in real-time kinetic investigations. The experimental approach for the study of dissociation of NC_{com} was simplified using a LS and this improvement makes it amenable for automation. The use of NC would also make the method more versatile extending its range to other types of ligands other than proteins.

1. Chaiken, I., Rose, S. and Karlsson, R., *Anal. Biochem.*, 1992, **201**, 197–210.
2. Malmquist, M., *Nature*, 1993, **361**, 186–187.
3. Murthy, G. S. and Venkatesh, N., *J. Biosci.*, 1996, **21**, 641–651.
4. Murthy, G. S., *Curr. Sci.*, 1996, **71**, 981–988.
5. Murthy, G. S., *Curr. Sci.*, 1997, **73**, 1097–1103.
6. Murthy, G. S., Lakshmi, B. S. and Moudgal, N. R., *J. Biosci.*, 1989, **14**, 9–20.
7. Venkatesh, N., Nagaraja and Murthy, G. S., *Curr. Sci.*, 1995, **69**, 48–58.
8. Fraker, P. J. and Speck, J. C., *Biochem. Biophys. Res. Commun.*, 1978, **80**, 849–857.
9. Pellequer, J. L. and Ven Regenmortel, M. H. V., *J. Immunol. Methods*, 1993, **166**, 133–143.
10. Kalinin, N. L., Ward, L. D. and Wrizor, D. J., *Anal. Biochem.*, 1995, **228**, 238–244.
11. Johne, B., Gadnell, M. and Hansen, K., *J. Immunol. Methods*, 1993, **160**, 191–198.
12. Mackonzie, C. R., Hirana, T., Deng, S. J., Bundle, D. R., Narang, S. A. and Young, N. M., *J. Biol. Chem.*, 1996, **271**, 1527–1533.
13. Malmborg, A. and Borrebaeck, C. A. K., *J. Immunol. Methods*, 1995, **183**, 7–13.

ACKNOWLEDGEMENTS. We thank the Department of Science and Technology and Technology Development Mission for their financial assistance.

Received 26 November 1999; revised accepted 11 April 2000

Mitogenic and melanogenic activity of human placental protein/peptides on melanoma cell

Samir Kumar Mandal[‡], Shampa Mallick[‡], P. K. Dutta[†] and Ranjan Bhadra[‡,*]

[‡]Department of Cellular Biochemistry, Indian Institute of Chemical Biology, 4, Raja S.C. Mullick Road, Jadavpur, Calcutta 700 032, India
[†]Department of Medicine, Dermatology Unit, Calcutta Medical College, Calcutta 700 073, India

An alcoholic extract of the term human placenta, when resolved into a protein/peptide component was found to show pigment and growth-inducing activity on B16F10 mouse melanoma cell *in vitro*. The protein/peptide component was studied in the dose range 0.01–100 µg/ml. At a concentration of 0.1 µg/ml, the growth of mouse melanoma was maximum, while the melanin formation was optimum at 50 µg/ml. Furthermore, the fraction markedly changes cellular morphology. Presence of ET-1 (endothelin-1) and ACTH (adrenocorticotropic hormone), two important melanocyte response modifiers was detected in the fraction. The activity of the protein/peptide fraction, in respect of morphology, pigmentation and growth, when compared with a mixture of pure ET-1 and ACTH reconstituted, at a level that is present in it, was found to be significantly higher.

MELANOGENESIS is a phenomenon associated with melanin pigment formation primarily in hair and skin of mammals[1]. Melanin, the dark brown pigment, is synthesized within membrane-bound organelles called melanosomes of the epidermal melanocyte cells. Among different bioactive proteins and peptides known to regulate melanogenesis, adrenocorticotropic hormone (ACTH)[2,3] and endothelin (ET)[4,5] have been reported in human placenta. ET though originally identified as a vasoconstrictive peptide, plays an important and regulatory role in mammalian pigmentation. Four mammalian ETs, namely ET-1, ET-2, ET-3 and big ET have been reported[6–8], though little information is available about their biological relevance, except ET-1. These peptides, produced and secreted by keratinocytes, act as strong mitogen[9,10], migration and dendricity inducer[11,12], and melanogen[13] for human melanocytes. ET also stimulates *mitogenesis in Swiss 3T3 fibroblast cell line*[14], renal mesangial cell[15] and vascular smooth muscle cells[16]. Mitogenic and melanogenic effects of ACTH on human melanocytes[17–19] and also in B16 melanoma cells[20] have also been reported in recent studies.

One prototype alcoholic extract prepared from human placenta of HIV and Hepatitis B negative mothers[21]

*For correspondence. (e-mail: iichbio@giascl01.vsnl.net.in)

showed pigment-inducing activity in mammals[22]. Its chemical analysis indicated the presence of numerous proteins/peptides and lipids, vitamins and other minor components including amino acids and nucleotides[23]. By fractionation of the extract, a placental protein peptide fraction (PPPF) was prepared.

In this report, we have attempted to estimate the content of ET-1 and ACTH, in the PPPF and investigate its effect on growth, pigmentation and morphology of B16F10 mouse melanoma cell *in vitro*.

Dulbuceo's Modified Eagle Medium (DMEM), Fetal Bovine Serum (FBS), 100X PSN Antibiotic and 10X Trypsin/EDTA solution were purchased from GIBCO BRL; standard synthetic melanin, [3-(4,5-dimethyl-thiazol-2-yl]-2,5-diphenyltetrazolium bromide (MTT), ET-1 and ACTH were from Sigma Chemical Co, St. Louis, USA; [^{3}H]Thymidine and ET-1 ELISA kit from Amarsham; Tissue Culture Plastic Wares from NUNC, Denmark; ACTH ELISA kit from Immunotech, France. All other chemicals used are of highest purity.

PPPF of hydroalcoholic human placental extract was prepared according to the method described previously[24]. Briefly, the dried mass of the hydroalcoholic human placental extract was treated with diethyl-ether at 4°C. Following centrifugation (2500 $g \times 10$ min at 4°C), the pelleted matter was identically treated thrice. The process was repeated three more times with ethanol–ether (3:1 v/v). The resultant pellet was dried completely and solubilized in distilled water and taken as PPPF.

ET-1 and ACTH were determined by ELISA kit, as per the manufacturers protocol.

In this study, we used B16F10 mouse melanotic cell line, procured from National Centre Cell Science, Pune, India. It was maintained in 10% FBS-DMEM medium with 1% PSN antibiotic and cultured weekly at 37°C with a humidified atmosphere of 5% CO_2 and 95% air. All experiments were conducted in DMEM containing 2% heat inactivated FBS and 1% PSN antibiotic.

Melanin was estimated as reported earlier[25]. Briefly, B16F10 melanoma cells were seeded in 6-well TC-plates at a density of 10^5 cells/well and cultured for 24 h. Following treatment with the stimulants for stipulated periods, the cells were trypsinized, harvested, counted, pelleted and dissolved in 1 ml of 1 N NaOH to measure the absorbance at 475 nm. The melanin content was calculated from a standard curve of synthetic melanin (Sigma).

[^{3}H]Thymidine incorporation was studied in B16F10 mouse melanoma cells according to Komori *et al.*[26]. Briefly, 10^4 cells/well were seeded in 96-well TC-plates, cultured with the stimulants for 24 h and then pulsed with 1 µCi/ml ^{3}H-Thymidine (sp. activity 6.70 Ci/nmol) for 6 h prior to harvesting. Finally, cells were harvested using Nunc-cell harvester and radioactivity incorporated was then determined by liquid scintillation counter (Model: LKB Wallac 1209 RACK BETA).

MTT cytotoxicity assays were performed as described earlier[27]. Briefly, 10^4 cells/well were plated in 96-well TC plates. After required incubation with the stimulants for 48 h, MTT solutions were added and the insoluble derivative formed by cellular dehydrogenase enzymes was solubilized with acidic isopropanol and absorbance was measured at 570 nm.

Quantitative estimation of PPPF was done by Lowry method[28] using bovine serum albumin as standard.

The level of ET-1 and ACTH present in the PPPF is summarized in Table 1.

In normal culture medium of DMEM-10% FBS, B16F10 melanoma cells attach to the culture flask, spread out with large dendrites and form confluent monolayers within three days. When cells were cultured with 2% heat inactivated FBS, they grew slowly. These melanoma cells are lightly pigmented and less dendritic (Figure 1 *a*). Under identical growth conditions, if the growth medium was supplemented with PPPF, these cells showed multipolar, highly branched and enlarged dendritic network (Figure 1 *b*). Few centres of growing cell clusters with proliferative viable cells (as confirmed by Trypan Blue Dye exclusion test), appeared in places of the monolayer culture. All cells showed the presence of dense pigmented granules in the cytoplasm. On the other hand, standard mitogens, ET-1 and ACTH at a concentration equivalent to what was present in PPPF did not produce any significant morphological change (Figure 1 *c*), when compared with the untreated cells. But at a comparatively high dose, ET-1 and ACTH showed marked morphological change (Figure 1 *d*) with extended dendricity, mainly bipolar in nature and granular pigmented cytoplasm.

We have investigated the stimulation of growth using PPPF, ET-1 and ACTH by [^{3}H]Thymidine incorporation to compare the results. Growth stimulation by PPPF was observed throughout the concentration range of 0.01–50 µg/ml, with maximum stimulation up to a level of 157.6% at a concentration 0.1 µg/ml. However, at concentrations higher than 50 µg/ml, growth was inhibited, though the cells remained viable (as judged by MTT assays). Table 2 shows comparison of growth induction by PPPF along with standard mitogens ET-1 and ACTH. Nanomolar doses of pure ET-1 and ACTH, a concentration much higher than what was present in 0.1 µg/ml of PPPF, failed to elicit the response induced by PPPF.

Table 1. Quantitative estimation of mitogenic factors (ET-1 and ACTH) in PPPF

Mitogenic agent	Amount detected
ET-1	50 ± 5 fmol/ml ET-1 per 100 µg PPPF*
ACTH	1.21 ± 0.11 fmol/ml ACTH per 100 µg PPPF*

Values are mean ± SE from triplicate sets.
*Yield of PPPF: 100 ± 10 µg PPPF per ml of crude placental extract.

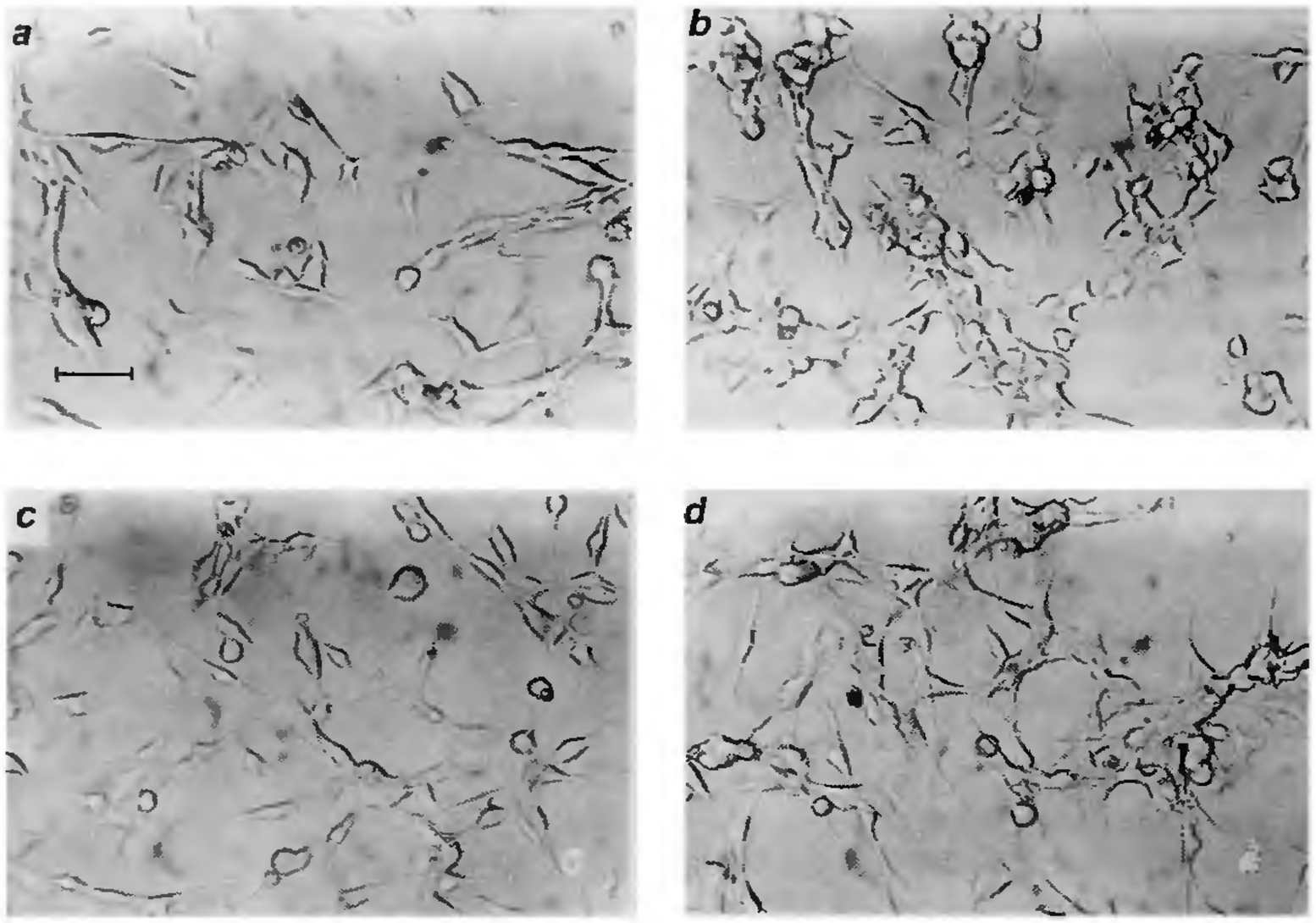

Figure 1. Morphological change for 2-day-old culture of B16F10 mouse melanoma cells. Untreated cells (*a*), cells treated with 10 µg/ml of PPPF (*b*), with 5 fM/ml ET-1 and 0.12 fM/ml ACTH (amount equivalent to that present in 10 µg/ml PPPF) (*c*) and mixture of 5 nM ET-1 and 5 nM ACTH (*d*). bar represents 50 µm. All photographs are under equal magnification.

Melanin production is an inherent phenomenon of B16F10 mouse melanotic melanoma cell line. The melanogenic effect of PPPF, studied over a wide concentration range from 0.1 µg to 100 µg/ml showed melanization in a concentration-dependent manner. An optimum melanin level of 139.7% (5.49 ± 0.11 µg melanin/10^5 cells) compared to untreated (control) cells (3.90 ± 0.09 µg melanin/10^5 cells) was observed at 50 µg/ml PPPF, a dose found non-cytotoxic by MTT assay. However, PPPF at 100 µg/ml, a dose much higher than 50 µg/ml, showed a marginal rise in melanin level, but the growth induction was inhibited compared to 50 µg/ml (Tables 2 and 3). Growth and melanin formation, when compared were found most compensatory at 50 µg/ml of PPPF and hence this dose was considered optimum for pigmentation. Table 3 shows a comparative study of melanization by ET-1 and ACTH along with PPPF. Even at nanomolar concentrations, these bioactive peptides either alone or in combination were not effective enough for melanin formation as observed with 50 µg/ml PPPF.

Table 2. Effect of PPPF, ET-1 and ACTH on [^{3}H]Thymidine incorporation in B16F10 melanoma cells

Stimulant	Radioactivity incorporated per 1.2×10^4 cells
Control	2842 ± 190
0.001 µg/ml PPPF	3276 ± 210
0.01 µg/ml PPPF	3711 ± 199
0.1 µg/ml PPPF*	4481 ± 239
1.0 µg/ml PPPF	3680 ± 208
10 µg/ml PPPF	3453 ± 186
25 µg/ml PPPF	3023 ± 260
50 µg/ml PPPF	2989 ± 204
100 µg/ml PPPF	2319 ± 216
0.5 fM/ml ET-1 + 0.012 fM/ml ACTH (equivalent amount of ET-1 and ACTH, present in 0.1 µg/ml PPPF)	2849 ± 239
1 nM ET-1	3098 ± 248
10 nM ET-1	3167 ± 198
1 nM ACTH	3234 ± 264
10 nM ACTH	3478 ± 211
1 nM ET-1 + 1 nM ACTH	3569 ± 236
10 nM ET-1 + 10 nM ACTH	4329 ± 202

Values are mean ± SE from triplicate determinations.
*Maximal mitogenic dose of PPPF.

Table 3. Comparison of melanin biosynthesis by PPPF, ET-1 and ACTH on B16F10 mouse melanoma cells

Stimulant	Melanin (in μg) per 1×10^5 cells
Control	3.90 ± 0.09
0.1 μg/ml PPPF	4.37 ± 0.08
1.0 μg/ml PPPF	4.28 ± 0.14
10 μg/ml PPPF	4.51 ± 0.10
50 μg/ml PPPF*	5.49 ± 0.11
100 μg/ml PPPF	5.65 ± 0.15
25 fM/ml ET-1 + 0.6 fM/ml ACTH (synthetic ET-1 and ACTH at an amount equivalent to that present in 50 μg/ml PPPF)	3.93 ± 0.12
1 nM ACTH	4.10 ± 0.10
10 nM ACTH	4.79 ± 0.11
1 nM ET-1	3.99 ± 0.14
10 nM ET-1	4.27 ± 0.15
1 nM ET-1 + 1 nM ACTH	4.41 ± 0.11
10 nM ET-1 + 10 nM ACTH	5.35 ± 0.13

Values are mean ± SE.
*Optimal melanogenic dose.

In this study the protein–peptide fraction was found highly effective in modulating the activity of B16F10 mouse melanoma cell *in vitro*. Among the known bioactive peptides capable of melanoma/melanocyte activity modulation, ET-1 and ACTH were found in measurable amounts in PPPF. Hearing *et al.*[17] reported that minimal dose of ACTH for mitogenic activity was 0.1 nM. The concentration of ACTH present in 0.1 μg PPPF, the optimal mitogenic dose, was 0.012 fM, significantly lower than the reported minimal dose of 0.1 nM. Again *in vitro* mitogenic and melanogenic activities of the bioactive peptide ET-1 were reported in the dose range of 1–10 nM (ref. 9), a level much higher than that detected in PPPF. However ACTH and ET-1 were found active at 1 nM and 10 nM concentrations, such response was enhanced when both bioactive peptides were added together (Tables 2 and 3). The growth and pigmentation of melanocytes relate inversely, and this was supported by the results of PPPF. At higher concentrations, the suppression of growth was indicative of stress generated due to PPPF, and stress-specific melanization events were reported by Gilchrest, Eller and Oslram[29]. Morphological changes of melanoma cells as observed by light microscope bore great significance. Pigment recovery in vitiligo, besides growth and melanization of melanocytes, was reported to be associated with morphological changes[30], and this study showed clearly that mitogenic and melanogenic response modifier PPPF was effective in changes in cellular morphology. In varieties of cell types, regulation of cell dendricity was reported to be associated with morphological changes[31,32]. So PPPF was found active for the modulation of growth, pigmentation, morphological change, including dendricity of B16F10 melanoma.

This study thus demonstrated that response of B16F10 melanoma to the placental protein peptide fraction from an alcoholic extract of human placenta did not correlate with the action of ET-1 and ACTH in respect of their concentration. Therefore additional components present in PPPF might act either synergistically with ET-1 and ACTH or directly to modulate the melanoma response. Under various stages and conditions, the response modification of melanoma by the protein–peptide fraction, appeared to be highly corroborative with the activity modulation of melanocyte necessary in pigment recovery.

1. Imokawa, G., Yada, Y. and Hori, Y., *J. Invest. Dermatol.*, 1988, **91**, 106–113.
2. Liotta, A., Osathanondh, R., Ryan, K. J. and Krieger, D. T., *Endocrinology*, 1977, **101**, 1552–1558.
3. Shibasaki, T., Odagari, E., Shizume, K. and Ling, N., *J. Clin. Endrocrinol. Metab.*, 1982, **55**, 384–386.
4. Malasine, A., Cronier, L., Mondon, F., Mignot, T. M. and Ferre, F., *Cell Tissue Res.*, 1993, **271**, 491–497.
5. Barry, M. W., Myron, S. and Peter, F. M., *J. Histochem. Cytochem.*, 1993, **41**, 535–541.
6. Yanagisawa, M., Kurihara, H., Kimura, S., Tomobe, Y., Kobayashi, M., Mitsui, Y., Yazaki, Y., Gato, K. and Masaki, T., *Nature*, 1988, **332**, 411–415.
7. Inoue, A., Yanagisawa, M., Kimura, S., Kasuya, Y., Miyaucho, T., Gato, K. and Masaki, T., *Proc. Natl. Acad. Sci. USA*, 1989, **86**, 2863–2867.
8. Sigiura, M., Snajdar, R. M., Schwartzberg, M., Badr, K. F. and Inagami, T., *Biochem. Biophys. Res. Commun.*, 1989, **162**, 1396–1401.
9. Yada, Y., Higuchi, K. and Imokawa, G., *J. Biol. Chem.*, 1991, **266**, 18352–18357.
10. Imokawa, G., Yada, Y. and Miyagishi, M., *J. Biol. Chem.*, 1992, **267**, 24675–24680.
11. Horikawa, T., Norris, D. A., Yohn, J. J., Zekman, T., Travers, J. B. and Morelli, J. G., *J. Invest. Dermatol.*, 1995, **104**, 256–259.
12. Hara, M., Yaar, M. and Gilchrest, B. A., *J. Invest. Dermatol.*, 1995, **105**, 744–748.
13. Imakawa, G., Yada, Y. and Kimura, M., *Biochem. J.*, 1996, **314** 305–312.
14. Takuwa, N., Takuwa, V., Yanagisawa, M., Yamashita, K. and Masaki, T., *J. Biol. Chem.*, 1989, **264**, 7856–7861.
15. Simonson, M. S., Wann, S., Mene, P., Dubyak, G. R., Kester, M., Nakazato, Y., Sedor, J. R. and Dunn, M. J., *J. Clin. Invest.*, 1989, **83**, 708–712.
16. Nakai, T., Nakayama, M., Yamamato, S. and Kato, R., *Biochem. Biophys. Res. Commun.*, 1989, **158**, 880–883.
17. Malek, Z. A., Swope, V. B., Suzuki, I., Akeali, M. D., Harringer, M. D., Boyce, S. T., Urabe, K. and Hearing, V. J., *Proc. Natl. Acad. Sci. USA*, 1995, **92**, 1789–1793.
18. Hunt, G., Todd, C., Kyne, S. and Thody, A. J., *J. Endrocrinol.*, 1994, **140**, R1–R3.
19. Hunt, G., Todd, C., Kyne, S. and Thody, A. J., *J. Endocrinol.*, 1993b, **139** (suppl), 29.
20. Lunec, J., Pieron, C. and Thody, A. J., *Melanoma Res.*, 1992, **2**, 5–12.
21. Bhadra, R., Pal, P., Roy, R. and Dutta, A. K., US patent No. 5690966, European patent application no. 96308000.7-2107, Indian patent application no. 1228/Del/94, Japaneese patent pending.
22. Manuscript communicated.

23. Pal, P., Roy, R., Dutta, P. K., Biswas, B. and Bhadra, R., *Int. J. Dermatol.*, 1995, **34**, 61–66.
24. Osborne, J. C. (Jr.), *Methods Enzymol.*, 1986, **128**, 213–222.
25. Naeyaert, J. M., Eller, M. Gardon, P. R., Park, H. Y. and Gilchrest, B. A., *Br. J. Dermatol.*, 1991, **125**, 297–303.
26. Komori, H., Ichikawa, S., Hirabayshi, Y. and Ito, M., *J. Biol. Chem.*, 1999, **274**, 8981–8987.
27. Mossman, T., *J. Immunol. Methods*, 1983, **65**, 55.
28. Lowry, O. H., Rosebrough, N. J., Farr, A. L. and Randall, R. J., *J. Biol. Chem.*, 1951, **193**, 265–275.
29. Gilchrest, B. A., Eller, M. S. and Oslram, K., *Proc. Natl. Acad. Sci. USA*, 1996, **93**, 1087–1092.
30. Cui, J., Shen, L. and Wang, G., *J. Invest Dermatol.*, 1991, **97**, 410–416.
31. Edwards, J. G., Campbell, C., Carr, M. and Edward, C. C., *J. Cell. Sci.*, 1993, **104**, 399–407.
32. Preston, S. F., Volpi, M., Pearson, C. M. and Berlin, R. D., *Proc. Natl. Acad. Sci. USA*, 1987, **84**, 5247–5251.

ACKNOWLEDGEMENTS. We thank the Director, IICB, for his kind interest; Mrs B. Das and Mr R. Bera for technical help and the unknown reviewer for his/her active interest. S.K.M. thanks DST and NES, Govt. of West Bengal and S.M. thanks DBT, Govt. of India for financial support.

Received 24 January 2000; revised accepted 11 April 2000

Identification of probable faults in the vicinity of Harnai–Ratnagiri region of the Konkan coast, Maharashtra, India

Biswaketan Kundu* and Anand Matam

Department of Earth Sciences, Indian Institute of Technology Bombay, Mumbai 400 076, India

The Konkan coastline from Harnai to Guhagar consists of many straight line segments being arranged in an en-echelon manner. The false color composite (FCC) reveals the coincidence of these segments with NW–SE trending lineaments that conspicuously cut across the Deccan Basalt Province adjoining the seacoast. Furthermore, another less prominent lineament set has been noticed in ENE–WSW direction offsetting the former. These lineaments are occupied by major rivers which originate from the Western Ghats escarpment and flow westerly into the Arabian Sea. Trellis and barbed type of drainage pattern are observed due to strong influence of these sets of lineaments. One of the NNW–SSE lineaments extending from Harnai to Kajurli has been studied, which reveals the presence of narrow and straight course of river flowing along it. While the western bank of the river is steep with a number of waterfalls, the eastern side carries flat terraces. The riverbed exposes highly fractured basalt criss-crossed by NNW–SSE and ENE–WSW sets of fractures. The NNW–SSE set which is sympathetic to the main lineament, hosts quartz veins that show pinch-and-swell and boudinage structure. The boudins are sigmoidal and are arranged in en-echelon pattern indicating shear origin. Hence it is believed that the NNW–SSE lineaments are probable faults in the area. Rare slickensides are observed on the quartz vein wall, which are mostly subvertical, suggesting a dip slip nature of faulting. The faulting is post-Deccan Basalt and could be Quaternary in age.

THE Deccan Trap forms one of the major fissure eruption provinces of Upper Cretaceous–Eocene age, covering an area of about 500,000 km^2 of the Indian Peninsula. It extends from central and western to the Arabian Sea and probably to Seychelles. The coastal geomorphology of West Coast of India is greatly controlled by the tectonics of the Deccan Volcanic Province (DVP). The structural framework of the DVP, along the West Coast, has been studied in great detail by many researchers. The important structural features include (1) The NW–SE trending West Coast fault[1–5], (2) N–S trending West Coast anticline[6–10], (3) Western Ghats escarpment[1,11–16], (4) Panvel flexure[18–24] and many NW–SE and E–W trending lineaments. The south-western DVP is dominated by NW–SE lineaments which are considered to be the transmission of the northwesterly structure of Dharwar-craton which presumably underlies the basaltic province[15,10]. These megastructures have probably originated due to uplift and rifting of the Western Passive Continental Margin[26]. Though these lineaments are considered to be faults, convincing field criteria to support such conclusion are, however, lacking. In this paper an attempt has been made to evaluate these lineaments on the basis of detailed structural analysis. The study area lies to the west of the Western Ghats escarpment between Harnai and Guhagar (Toposheet No. 47 G/1–4 and 8, 7) in the Ratnagiri district of Maharashtra (Figure 1).

The study area is marked by undulating hills. The hills are made up of horizontal basaltic lava flows with flat lateritic capping. The coastal line is remarkably straight with a few land protrusions into the sea. The beaches are very narrow and are characterized by vertical cliffs with flat rock beds. Vashishti and Shastri are two major rivers in the area, which originate from the Western Ghats escarpment and flow westerly into the Arabian Sea. The rivers are marked by right angle bends. Many tributaries meet these rivers at right angle, sometimes forming barbed joins.

The study of the IRS 1C LISS III FCC(532) reveals that the NNW–SSE trending coastline is the major linear feature in the area (Figure 2). Detailed analysis reveals that the coastline consists of many long northwesterly

*For correspondence. (e-mail: kundu@geos.iitb.ernet.in)